JOURNAL OF APPLIED STATISTICS
2023, VOL. 50, NO. 16, 3229–3250
https://doi.org/10.1080/02664763.2022.2104822

Taylor & Francis
Taylor & Francis Group

Check for updates

Spatio-temporal modeling of traffic accidents incidence on urban road networks based on an explicit network triangulation

Somnath Chaudhuri [a], Pablo Juan [a,b] and Jorge Mateu [c]

[a]Research Group on Statistics, Econometrics and Health (GRECS), University of Girona, Girona, Spain; [b]IMAC, University Jaume I, Castellón, Spain; [c]Department of Mathematics, University Jaume I, Castellón, Spain

ABSTRACT

Traffic deaths and injuries are one of the major global public health concerns. The present study considers accident records in an urban environment to explore and analyze spatial and temporal in the incidence of road traffic accidents. We propose a spatio-temporal model to provide predictions of the number of traffic collisions on any given road segment, to further generate a risk map of the entire road network. A Bayesian methodology using Integrated nested Laplace approximations with stochastic partial differential equations (SPDE) has been applied in the modeling process. As a novelty, we have introduced SPDE network triangulation to estimate the spatial autocorrelation restricted to the linear network. The resulting risk maps provide information to identify safe routes between source and destination points, and can be useful for accident prevention and multi-disciplinary road safety measures.

ARTICLE HISTORY
Received 22 December 2021
Accepted 9 July 2022

KEYWORDS
INLA; network triangulation; Poisson hurdle model; SPDE; traffic risk mapping

1. Introduction

Road traffic collisions is one of the serious issues in the modern world. According to 2018 global status report on road safety by the World Health Organisation, approximately 1.35 million people die each year as a result of traffic collisions [74]. The rate of occurrence along with severity of traffic crashes are the principal indicators of urban road safety measures [74]. Literature suggests that factors such as road infrastructure or types of roads (highways, double or, single carriage tracks) play a vital role in road safety measures [18]. Indeed, uncontrolled vehicle speed or street junctions without traffic signals increase accident risk [10], but temporal factors (time of the day or weekend nights) also act as decisive aspects in the count and impact of accidents [20,33]. Identifying such significant elements has been a central focus of research in the domain of road safety. Available map applications offered by larger corporations, such as Google Maps or collaborative geospatial projects (for example, OpenStreetMap (OSM)) can provide information about the fastest (shortest) route from source to destination points. The existing applications can suggest,

CONTACT Pablo Juan juan@uji.es

Supplemental data for this article can be accessed online at https://doi.org/10.1080/02664763.2022.2104822.

© 2022 Informa UK Limited, trading as Taylor & Francis Group

however, the shortest route without considering likely risk factors. Multi-disciplinary predictor aspects are not implemented in most of these applications. According to Williamson and Feyer [76], a particular road can be safe during mid-day, but the same road might not be safe during office hours. Relevant spatio-temporal factors play a significant role in identifying safe roads [52]. Traffic components such as street light, road type, or speed limits act as significant factors in determining safe routes [12,44]. Thus, a multi-disciplinary approach is essential to explore spatio-temporal effects on road collisions. Identifying significant components [19,60] while performing spatio-temporal modeling of traffic accidents [30,78] have gained an increasing interest in the domain of road safety management. Research works by [5,6,44] made notable contributions in identifying significant factors influencing traffic collisions. Bhawkar [8] explored and analyzed the leading factors causing road accidents on the streets of UK. Shahid *et al.* [63] mentioned that the causes of traffic collisions can be broadly classified into spatial and temporal components. A series of studies [3,20,26,62] analyze historic data to identify risk factors and assess likelihoods of crash-related events to categorize spatio-temporal factors affecting traffic accidents. These factors are considered as significant predictors in statistical analysis and prediction modeling.

Several statistical techniques such as Poisson model variations [13,37,42,49], negative binomial error structure [53], logistic [28] and linear regressions [1] have been applied to analyze spatial variability of traffic accidents. In this regard, Wang *et al.* [72] while analyzing factors influencing traffic accident frequencies on urban roads, mentioned that accidents occurring at different locations are related. It supports spatial autocorrelation of traffic accident events. Spatial methods are able to incorporate geographical correlation in the model fitting process and, in most of the cases, spatial methods outperform the non-spatial models [23,77]. In this line, a number of research works [27,29,30,35] suggest that stochastic spatial processes are one of the most appealing analytical tools to analyze the spatial and spatio-temporal distribution of traffic collisions. Karaganis and Mimis [29] used spatial point processes to evaluate the probability of traffic accident occurrence on the national roads of Greece. In this context, statistical inference comes along with Bayesian methodology. Cantillo *et al.* [12] used a combined GIS-empirical Bayesian approach in modeling traffic accidents on the urban roads of Colombia. A space-time multivariate Bayesian model was designed by Boulieri *et al.* [21] used Bayesian spatial modeling with INLA in predicting road traffic accidents based on unmeasured information at road segment levels. The use of INLA-SPDE for spatial data is now quite well established in a number of disciplines with a large number of contributions [7,25,70] and in particular the references therein. However, in the context to traffic accident event modeling, there are limited contributions implementing Bayesian methodology with INLA-SPDE approach. In addition, if we consider events with a network support, see [14,45,46] for a nice overview of spatial and spatio-temporal point pattern analysis on linear networks, then Bayesian methodology on road networks using INLA-SPDE is even far under explored.

The aim of this paper is two-fold. On one side we provide a modeling framework to explore and analyze the spatial and temporal variation in the incidence of road traffic accidents on individual road segments. The second aim roots in providing an advanced and realistic computational strategy to create the spatial triangulation restricted only onto the network topology. In this context, we propose the novel concept of multi-disciplinary road-safety analysis by introducing spatio-temporal risk modeling of traffic accidents using

Bayesian methodology restricted entirely onto the road network. Our model acts as a comprehensive scoring system that can predict a risk index over individual road segments generating a categorized risk map of the entire road network. The study is conducted on five years road traffic accidents data from the city of London, UK. R programming language (version R 4.0.4) has been used for statistical computing and graphical analysis. All computations are conducted on a quad-core Intel i7-4790 (3.60 GHz) processor with 32 GB (DDR3-1600) RAM.

The rest of the paper is organized as follows. Section 2 presents the OSM street network data and provides some insights of the spatial distribution of traffic accidents in the city of London, UK. A description of the spatio-temporal modeling framework comes in Section 3. The design of the risk map algorithm is discussed in Section 3.2. Section 4 is devoted to present the results of model prediction and risk map analysis. Some discussion and concluding remarks come in Section 5.

2. Data settings

The Department for Transport of the Government of UK publishes road casualty statistics twice a year. Detailed data about the circumstances of road accidents on public roads reported to the police, and the corresponding casualties, are recorded using the STATS19 accident reporting form. The complete data set since 1979 is available in the UK Government open data repository [69]. The data is free and available under the *Open Government Licence v3.0* for public sector information. The dataset used in this paper contains detailed information of traffic accidents for five years, from January 2013 to December 2017, that have occurred in the city of London, UK. The city has an area of 2.90 km^2, comprises six Lower Layer Super Output Area (LSOA) with an approximate population of around 90,000 citizens. The area is an important local district that contains the historic center and the primary Central Business District (CBD) of London.

According to Prasannakumar [52] the number of traffic collisions in each road segment plays a key role in designing predictive models that can reflect the influence of spatio-temporal factors on traffic accidents. The original traffic accidents dataset retrieved from [69] has records of daily accidents with geographical coordinates of individual occurrence. But one of the principal objectives of the current study is to measure the risk factor of individual road segments in the study area. As a result, we have applied up-scaling methods on both temporal and spatial resolutions. To identify the risk status of respective road segments rather than checking individual locations of accidents, the spatial resolution has been up-scaled to road networks, and the temporal unit is considered as month, to avoid having extreme number of zero-counts per segment. Thus, our target variable is the total number of accidents occurring in each road segment per month, from 2013 to 2017. An individual year will have $12 \times 1406 = 16872$ events, where 1406 is the number of road segments in the entire study area. This results in $5 \times 16872 = 84360$ events for five years of the study period on all road segments. We note that in 98% of the cases, we have no monthly traffic accidents on any road segment, and only 2% shows monthly accident records ranging from 1 to 4. Figure 1(left) illustrates the frequency distribution of instances with no accidents (depicted as zero) and more than one accident, and Figure 1(right) depicts the frequency distribution of only non-zero instances.

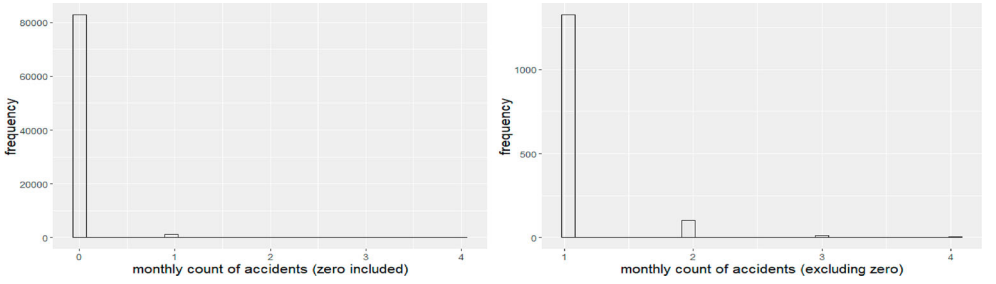


Figure 1. Frequency distribution of monthly instances with (*left*) no accidents (depicted as zero) and other values, and (*right*) only non-zero instances on all road segments in the study area.



Figure 2. OSM street network with locations of traffic accident (2013–2015) highlighted in gray.

The road network is accessed from OSM repository using R package osmdata [51]. OSM data is free and licensed under the *Open Data Commons Open Database License (ODbL)* by the OpenStreetMap Foundation. The OSM street network is illustrated in Figure 2, noting that OSM highway categories such as unclassified, bus_guideway, raceway, path and bridleway are not included. Figure 2(right) also depicts individual accident locations (highlighted in red) over 1406 road segments in the OSM network.

We report that in the model fitting process we have used three covariates such as road type, road surface and months of a year. According to Transport for London [69], road surface has five unique categories such as dry, wet, snow, frost and flood (where surface water is over 3 cm deep). On the other hand, road types are roundabout, one way street, dual carriageway, single carriageway and slip road. The variable month ranges from 1 to

12. All three covariates are used as factors in the model. We note that for model fitting we have used traffic accident records for three years (January 2013 to December 2015) have been used while the records of following two years (January 2016 to December 2017) have been used for prediction purposes.

3. Spatio-temporal modeling

Random spatial events, such as traffic accidents, form irregularly scattered point patterns over regions of interest. In these cases, spatio-temporal point process models are useful tools to perform focused statistical analysis [27,29,35]. Moreover, we can consider that these events exist on a linear network, and we can find recent literature [21,45,46] on spatio-temporal point processes over networks that are able to identify spatial autocorrelations and interactions between points in the pattern. In this context, it is shown that the occurrence of traffic accidents depend on spatio-temporal interacting and triggering factors [34].

By aggregating data from locations to counts of events per segment, we open the door to consider Poisson regression models in combination with a Bayesian framework for the prediction of traffic accidents on individual road segments. A Bayesian approach with Markov Chain Monte Carlo (MCMC) simulation methods can be used to fit generalized linear mixed models (GLMM) [75]. MCMC methods provide multivariate distributions that can estimate the joint posterior distribution. As mentioned in Section 1, for latent Gaussian models and models having a large number of geo-locations, the performance of MCMC methods drops substantially [57,66,68]. As an alternative and computationally faster solution, prediction of marginal distributions by using a Laplace approximation for integrals was introduced by Rue *et al.* [57] with the integrated nested Laplace approximation (INLA) method. It focuses on models that can be expressed as latent Gaussian Markov random fields (GMRF) [56].

We indeed follow this approach combining a spatio-temporal Poisson regression method within a Bayesian framework using INLA and SPDE. In particular, let Y_{it} and E_{it} be the observed and expected number of road traffic accidents on the i-th road segment and at the t-th month, $t = 1, \ldots, T$. We assume that conditional on the relative risk, ρ_{it}, the number of observed events follows a Poisson distribution

$$Y_{it}|\rho_{it} \sim Po(\lambda_{it} = E_{it}\rho_{it})$$

where the log-risk is modeled as

$$log(\rho_{it}) = \beta_0 + Z_i^T\beta_i + \xi_i + \zeta_t + \epsilon_i + \delta_{it} \tag{1}$$

Here, ξ_i and ζ_t account for the spatially and temporally structured random effects, respectively, δ_{it} represents spatio-temporal interaction between the two structured effects, and ϵ_i stands for an unstructured zero mean Gaussian random effect and logGamma precision parameters 0.5 and 0.01, defined as penalized complexity (PC) priors [65]. Z_i represents the spatial covariates. We assigned a vague prior to the vector of coefficients $\beta = (\beta_0, \ldots, \beta_p)$ which is a zero mean Gaussian distribution with precision 0.001. All parameters associated to log-precisions are assigned inverse Gamma distributions with parameters equal to 1 and 0.00005. In the current study, we have chosen to provide default prior distributions for all parameters in R-INLA. These have been chosen partly based on priors

commonly used in the literature [9,41,47,58]. We report that our results are robust against other alternative priors, as we run several cases with different priors obtaining the same results.

Description of the dataset in Section 2 suggests the current model can have problems of instability, especially with spatial random effects, which would be exacerbated due to zero inflation. Apart from the baseline Poisson model, both zero-inflated Poisson (ZIP) and Poisson hurdle models can be formulated for zero inflated discrete distributions. They provide mixtures of a Poisson and Bernoulli probability mass function to allow more flexibility in modeling the probability of a zero outcome [2]. According to Lambert [31], ZIP models add additional probability mass to the outcome of zero. Poisson hurdle models, on the other hand, are characterized as pure mixtures of zero and non-zero outcomes [24,55,61]. In a ZIP model, the response variable is $Y_{it} = 0$ with probability π, and $Po(\lambda_{it})$ with probability $1 - \pi$. In particular,

$$Y_{it} = \begin{cases} 0 & \text{with prob } \pi + (1-\pi)e^{-\lambda_{it}} \\ k & \text{with prob } (1-\pi)\dfrac{\lambda_{it}^k e^{-\lambda_{it}}}{k!}, \quad k \geq 1 \end{cases}$$

On the other hand, a Poisson hurdle model indicates that $Y_{it} = 0$ with probability π, and a truncated Poisson distribution with parameter λ_{it} with probability $1 - \pi$. Thus, we have

$$Y_{it} = \begin{cases} 0 & \text{with probability } \pi \\ k & \text{with probability } \dfrac{(1-\pi)}{1-e^{-\lambda}} \left(\dfrac{\lambda_{it}^k e^{-\lambda_{it}}}{k!} \right), \quad k \geq 1 \end{cases}$$

In the model fitting process, we have explored three different distributions discussed above to fit the model in Equation (1). To compute the joint posterior distribution of the model parameters, we use an INLA-SPDE method, as introduced by Lindgren *et al.* [32]. SPDE consists in representing a continuous spatial process, such a Gaussian field (GF), using a discretely indexed spatial random process such as a Gaussian Markov random field (GMRF). In particular, the spatial random process ξ, here represented by $\xi()$ to explicitly denote dependence on the spatial field, follows a zero-mean Gaussian process with Matérn covariance function represented as

$$Cov(\xi(x_i), \xi(x_j)) = \frac{\sigma^2}{2^{\nu-1}\Gamma(\nu)} (\kappa ||x_i - x_j||)^{\nu} K_{\nu}(\kappa ||x_i - x_j||) \tag{2}$$

where $K_{\nu}(.)$ is the modified Bessel function of second order, and $\nu > 0$ and $\kappa > 0$ are the smoothness and scaling parameters, respectively. INLA approach constructs a Matérn SPDE model, with spatial range r and standard deviation parameter σ.

The parameterized model we follow is of the form

$$(\kappa^2 - \Delta)^{(\alpha/2)}(\tau S(x)) = W(x)$$

where $\Delta = \sum_{i=1}^{d} \frac{\partial^2}{\partial x_i^2}$ is the Laplacian operator, $\alpha = (\nu + d/2)$ is the smoothness parameter, τ is inversely proportional to σ, $W(x)$ is a spatial white noise and $\kappa > 0$ is the scale parameter, related to range r, defined as the distance at which the spatial correlation becomes negligible. For each ν, we have $r = \sqrt{8\nu}/\kappa$, with r corresponding to the distance

where the spatial correlation is close to 0.1. Note that we have $d = 2$ for a two-dimensional process, and we fix $\nu = 1$, so that $\alpha = 2$ in our case [9].

INLA-SPDE requires a triangulation or mesh structure to interpolate discrete event locations to estimate a continuous process in space [59]. We use centroids of each road segment as the target locations over which we build the mesh. A detailed description of building a Delaunay's triangulation with emphasis on a network mesh is shown in Section 3.1. Centroids of individual road segments and triangulations in the mesh are used to generate the projection matrix. Now we use *inla.spde2.pcmatern* function from R-INLA package to build SPDE model and specify PC priors for the parameters of the Matérn field. The parameters *prior.range* and *prior.sigma* control the joint prior on range and standard deviation of the spatial field [64,65]. According to Bakka *et al.* [7], the range value is selected based on the spatial distribution of event locations in the study area. In the current study, due to the proximity of accident locations we have decided to use a prior $P(r < 0.01) = 0.01$, which means that the probability that the range is less than 10 meters is very small. Parameter σ denotes the variability of the data. We specify the prior for this parameter as $P(\sigma > 1) = 0.01$.

On the other hand, the temporal random effect (ζ_t) is assumed to be a smoothed function, in particular a random walk of order one (RW1) [57]. Using the specifications discussed above, we design a set of models for three distributions such as Poisson, Poisson hurdle and ZIP. Each of these models are explored having different combinations of three covariates (mentioned in Section 2) and several choices amongst PC priors and default priors for the parameters to create a SPDE model object in case of a Matérn field. Details of each model are shown in Table 1 in Appendix. As reported in Equation (1), we have also introduced a spatio-temporal interaction effect as an independent unobserved term for each combination of region and period (i, t), thus without any structure $\delta_{it} \sim Normal(0, 1/\tau_\delta)$. However, if spatial and temporal main effects are present in the model, then this interaction only implies independence in the deviations from them. Note that it is a global space-time heterogeneity effect, and it is usually modeled as white noise [36]. See also Blangiardo and Cameletti [9]. Thus, a second set of models are designed using the three distribution types with all three covariates included in each case but with the choice of spatio-temporal interaction and PC priors. A summary of the considered competing models is depicted in Table 2 in Appendix.

As we have a battery of competing models, we compare them using the deviance information criterion (DIC) [67], which is a Bayesian model comparison criterion, represented as

$$DIC = \text{goodness of fit} + \text{complexity} = D(\overline{\theta}) + 2p_D$$

where $D(\overline{\theta})$ is the deviance evaluated at the posterior mean of the parameters, and p_D denotes the *effective number of parameters*, which measures the complexity of the model [67]. When the model is true, $D(\overline{\theta})$ should be approximately equal to the *effective degrees of freedom*, $n - p_D$. DIC may underpenalize complex models with many random effects.

An alternative is the Watanabe Akaike information criterion (WAIC) which follows a more strict Bayesian approach to construct a criterion [73]. Gelman *et al.* [22] claim that WAIC is more preferable over DIC. Likewise DIC, WAIC estimates the effective number of parameters to adjust over-fitting. *pWAIC* is similar to p_D in the original DIC. Gelman

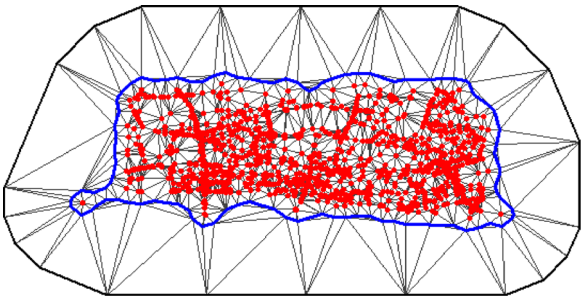


Figure 3. Selected region mesh with non-convex hull boundary.

et al. [22] scales the WAIC of Watanabe [73] by a factor of 2 so that it is comparable to AIC and DIC. WAIC is then reported as $-2(lppd - pWAIC)$ where *lppd* is the log pointwise predictive density and $pWAIC$ is the effective number of parameters. Therefore, the lowest values of DIC and WAIC suggest the best model. A high number of parameters means more complexity. The best models are those with a high level of complexity and a high goodness-of-fit. In general, we choose that model showing lower DIC and WAIC.

3.1. SPDE triangulation design

Due to the densely distributed nature of the road segments in the study area, initially a continuous spatial structure is chosen for modeling, and triangulation is carried out on the entire study area. Triangle size is generated using a combination of maximum edge and cut-off. The size controls how precisely the equations will be tailored by the data. Using smaller triangles increases precision but also exponentially increases computational time [70]. The best fitting mesh should have enough vertices for effective prediction, but the number should be within a limit to have control over the computational time. Following this principle, a series of meshes with varied range in the number of vertices are created. Finally, the best fitting mesh without offset value and having non-convex hull boundary is selected. The number of vertices in the selected mesh is 1526. Figure 3 depicts the selected mesh with the locations of traffic accidents (in red) during the time period of January 2013 to December 2017.

SPDE network triangulation: The mesh created for the entire region can be used to fit INLA model in the study area. Prediction involves projecting fitted model into the mesh at precise spatial locations. However, while fitting the mesh (as depicted in Figure 3) a problem appears. The sampled traffic accidents are discrete spatial points located precisely on the road networks, but models fitted with a region mesh cover the entire study area. Therefore, the predicted locations of traffic accident can be placed in any area with or without road networks. It is not realistic that the model prediction provides results in locations without road network where there is no chance of traffic accidents to occur. Thus, the traditional methods of model prediction using a region mesh are not useful. We need to introduce the novel idea of designing SPDE triangulation precisely on road networks. The process is executed following sequential steps where a buffer region for each road segment is initially created, next a clipped buffer polygon is constructed which comprises only the

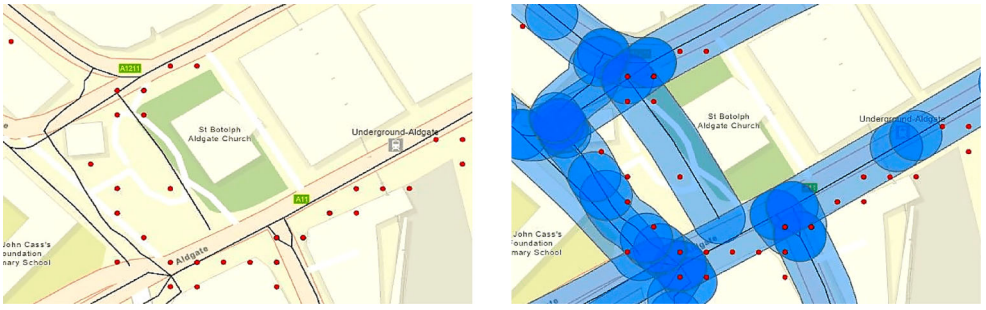


Figure 4. Traffic accident locations on road segments Without buffer (*left*), and With buffer (*right*).

area covered by the road network, and finally SPDE triangulation is applied on the clipped polygon to construct the *SPDE Network Mesh*. Each step of the network triangulation process is discussed in brief as follows.

Access OSM network: OSM road network for the study region is accessed using R package osmdata [51].

Buffer for each road segment: A report by the National Academies of Sciences, Engineering, and Medicine (USA) on quality and accuracy of positional data in transportation [48] highlighted accuracy and reliability issues of positional data in transportation research works. There are instances where recorded data entries invariably introduce errors in both geometric and contextual attributes [43]. This happens also with our road traffic accident data when being positioned over the extracted OSM road network. Figure 4(left) depicts a sample of traffic accident locations (marked as red points) on the OSM road network. We note that many events are located away from the road segments. Initially, the buffer width is selected in such a manner to get maximum points within a standard buffer area for all road segments. We report that the GPS error is very similar for all road segments irrespective of their individual width. Thus, a common selected buffer width for all road segments served the best to get maximum points within buffer area. So, we check out with different buffer widths common for all the road segments. We have used several buffers widths, and selected a 20 meters buffer as the optimal one where the maximum points lie within buffer regions for each road segments. In Figure 4(right) we show the built buffers using the function *geo_buffer* from R package stplanr [38]. OSM road network with 20 meters added buffer is depicted in Figure 5(left).

Create Clipped Buffer Polygon: Individual buffer segments are merged and converted into a single polygon clipped within a bounding box covering the study area. Figure 5(right) illustrates the clipped polygon of the buffered segments.

Apply network triangulation: As we need to analyze accident risk factor in each road segment, events within the buffer area of individual road segments are aggregated and counted. Then, the centroid of each segment is used as initial triangulation nodes applied on the clipped polygon. In relation to Delaunay's triangulation, it is worthy mentioning about the choice of buffer size and relevant parameters used to design SPDE mesh. Function *inla.mesh.2d* in R-INLA provides control for the largest allowed triangle edge length (*max.edge*) and minimum allowed distance between points (*cutoff*). The number of vertices in the SPDE mesh is regulated by both of these, as well as the boundary region of the study area. We report two issues while using buffer width proportional to street widths.



Figure 5. (*Left*) OSM road network with a 20 m buffer; (*Right*) Clipped polygon of buffered segments.

As mentioned in the previous section, erroneous GPS locations of accident sites leads to the first issue. In case of narrow streets, substantial numbers of accident points are found to be located outside the buffer area. The second issue is that when the buffer width goes below a threshold value, the entire structure of the mesh gets distorted. In contrast, if the buffer width is particularly large, owing to close proximity of road segments, two or more segments merge into one. This is not realistic in nature, especially while calculating the accident risk on individual road segments.

Thus, to avoid these technical issues we have identified a common threshold value for the buffer width for all road segments irrespective of their individual widths. According to Verdoy [70], we need to balance between number of vertices used to build the triangulated mesh and computational cost. The best fitting mesh should have enough vertices for effective prediction, but the number should be within a limit to have control over computational time. With this concept we have fine tuned *max.edge* and *cutoff* values with several models to identify the best fitted mesh. A series of SPDE-mesh are generated, and the best fitting mesh projected only on the road network, as illustrated in Figure 6, is selected. The number of vertices for the final selected mesh is 12666. Figure 6 depicts the network mesh together with 84360 accident events.

3.2. Risk map design

We discuss here how to build traffic accident risk maps onto the network structure coming from the fitted Poisson model. Coming from the predicted monthly accident occurrences on individual road segments, we build a *Risk Score* (R_{score}). Initially, the raw risk score for any road segment is equal to the sum of the total number of expected monthly accident counts for that segment. Then, we design a dynamic normalization technique to convert this raw risk into categorical values defining what we call a *Risk Index*. Finally, the normalized risk indices are adapted to design the risk map over the entire road network. These steps are detailed as follows.

In the current study, we have calculated the raw risk score for a road segment as the sum of monthly accident counts on that segment. Literature on road safety suggests that a predefined category range has to be decided before modeling any risk map [16]. Thus, we consider some sort of dynamic normalization technique for the raw risk scores. Initially,



Figure 6. Selected network mesh with added traffic accident locations.

Table 1. Normalization for risk index values.

Normalize condition	Risk index	Safety measure
Segment having zero R_{score}	0	Low risk
$R_{\text{score}} < R_{\text{range}}$	0	Low risk
$R_{\text{range}} \leq R_{\text{score}} < 2 \times R_{\text{range}}$	1	Low-medium risk
$2 \times R_{\text{range}} \leq R_{\text{score}} < 3 \times R_{\text{range}}$	2	Medium risk
$3 \times R_{\text{range}} \leq R_{\text{score}} < 4 \times R_{\text{range}}$	3	Medium-high risk
$4 \times R_{\text{range}} \leq R_{\text{score}}$	4	High risk

the risk range is calculated as follows

$$R_{\text{range}} = \frac{(\max . R_{\text{score}} - \min . R_{\text{score}})}{\text{no. of risk categories}} \tag{3}$$

Next, we have used R_{range} to calculate the normalized values. As a relevant example, the values depicted in Table 1 show that the number of categories in the normalized scale is the same as the proposed number of risk categories. We note that the proposed dynamic normalization technique can be applied to similar risk index scales in road safety management.

We also highlight that the safety measure mentioned in Table 1 follows the European Road Assessment Programme (EuroRAP) standard to create the risk ratings of the motorways and other national roads in Europe [54]. The risk index algorithm implemented here has intended to categorize road segments based on the traffic accident records in each segment. As a result, segments having higher accident counts are categorized as accident-prone or high risk roads. A similar methodology can be adapted in other traffic risk modeling algorithms. The Risk index values of individual road segments are adapted to design final risk maps.

4. Results

This section presents results of the analysis and methodological approach developed in Section 3. In particular, we provide results on model fitting and prediction together with risk maps of accidents.

4.1. Model fitting

The proposed model, mentioned in Equation (1) has been fitted to the accident datasets for the years 2013 to 2015. The remaining accident records of 2016 and 2017 have been used for prediction purpose. R-INLA package [41] is used to fit all models mentioned in Section 3, by adapting and modifying existing coding for space-time analysis [79]. All models are executed separately for the same data set (January 2013 to December 2015).

Deviance information criterion (DIC) and the Watanabe-Akaike information criterion (WAIC) are used to assess the performance of the models, and to select the best fitting model by balancing model accuracy against complexity [67]. Models having smaller DIC value, in spite of the added complexity, provide a more appropriate fit to the sampled data [9]. Summary results (DIC and WAIC) related to goodness-of-fit for all the fitted models are reported in Table 1 and Table 2 in Appendix. We note that, in each case, the computational time of non-interactive spatio-temporal models are found to be substantially low compared to the other interactive counterparts.

DIC values shown in Table 2 indicate that Poisson models (M1 to M4) provide the largest DIC values, while, in contrast, Poisson hurdle and ZIP show much better performances. Moreover, the zero-inflated models without spatio-temporal interaction (M5, M7, M9 and M11) provide a better fit than the corresponding spatio-temporal interactive pairs (M6, M8, M10 and M12). The values reported in Table 2 indicate that for model M7, DIC (9464.48) and WAIC (9471.32) are substantially lower compared to others.

Thus, to model the spatio-temporal structure of traffic accidents on London road networks, the Poisson hurdle model without a spatio-temporal interaction term is selected. We report that model M7 considers spatial and temporal effects together with three covariates (month, road type and surface) mentioned in Section 2. In each case, the models provide larger DIC and WAIC values when the covariates are not considered (see Table 1

Table 2. Competing models with DIC and WAIC values.

Model	DIC	WAIC
M1: Poisson	44137.41	44132.59
M2: Poisson	47251.88	47243.16
M3: Poisson	43433.75	43427.04
M4: Poisson	44041.93	44056.08
M5: Poisson hurdle	9571.01	9570.31
M6: Poisson hurdle	9932.40	9920.95
M7: Poisson hurdle	**9464**.48	**9471**.32
M8: Poisson hurdle	9490.83	9493.05
M9: Zero inflated Poisson	9683.70	9686.07
M10: Zero inflated Poisson	9896.62	9890.19
M11: Zero inflated Poisson	9491.44	9482.10
M12: Zero inflated Poisson	9511.15	9568.80

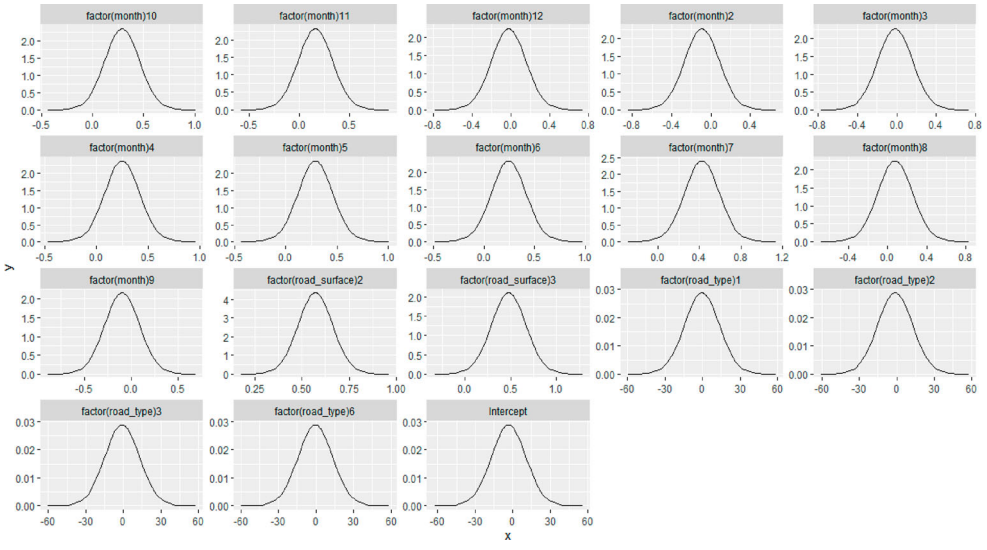


Figure 7. Marginal posterior distributions of covariate coefficients.

in Appendix). Additionally, the models perform better when PC priors are applied for the parameters to create the SPDE model object in case of Matérn model. As a note, in the current study, regardless of distribution type, the models show a better fit with the inclusion of all three covariates and PC priors under the case of no spatio-temporal interaction.

The posterior distribution of fixed and random effects included in the model are depicted in Figures 7 and 8. In particular, Figure 7 shows the marginal posterior distributions of all fixed effects related to covariates road type, road surface and month, confirming the Gaussian distribution centered at zero. Additionally, Table 3 in Appendix depicts the coefficients and credibility intervals of all fixed effects. We note that the covariate road type has no influence in our model. The positive mean values for the covariate road surface indicate positive influence in the model. However, in case of the month variable, only July shows positive significance while all other months have no influence in the model. In Section 5, we further detail the influence of variables on the model in further details.

Figure 8 depicts the marginal posterior mean of the spatial ξ_i and temporal ζ_t random effects. The horizontal axis of Figure 8 (top) represents 12666 triangulation nodes of SPDE network mesh used in the model. A stronger spatial effect is observed on the nodes of triangles on the road segments having higher accident counts (highlighted in Figure 6 as dark red patches). Similarly, Figure 8 (bottom) exhibits the variation of the marginal posterior mean of the temporal random effects over the 36 months for the model fitting years (2013 to 2015).

We finally note that spatial effect parameters κ and τ have mean values 162.53 and 0.2804 as depicted in Figure 9 that shows the marginal posterior distributions of the two hyperparameters for the spatial random field. Using κ and τ we can get the value of spatial range $r = 0.0174$ km or 17.4 m.

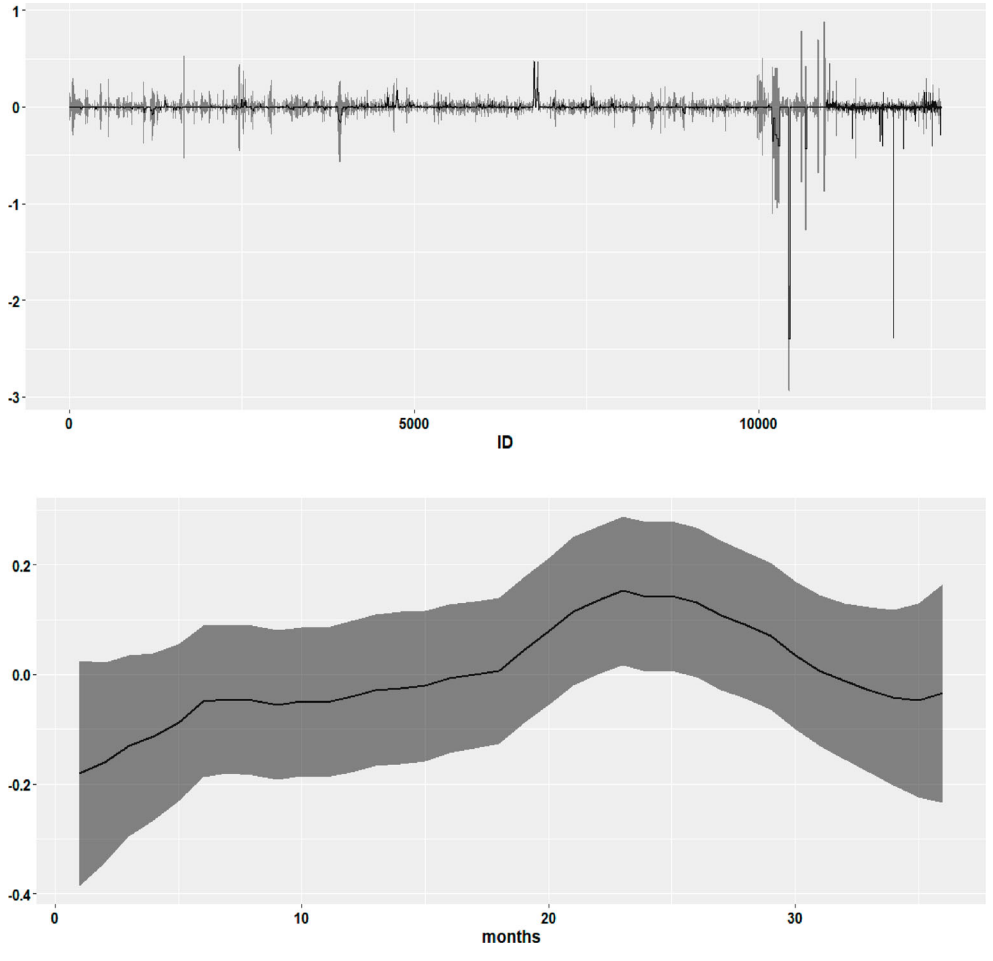


Figure 8. *Top*: marginal posterior mean of the spatial random effect $\xi(.)$; *Bottom*: marginal posterior mean of the temporal random effect ζ_t.

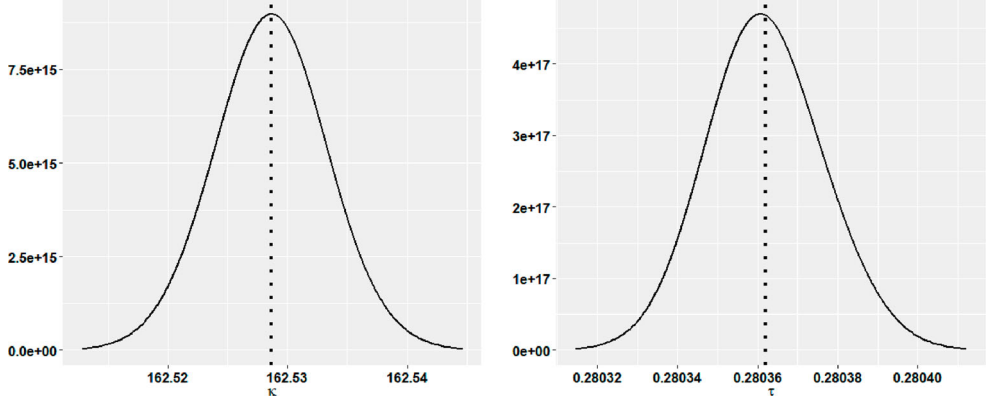


Figure 9. Marginal posterior distributions of hyperparameters κ and τ for the spatial random field $\xi(.)$.

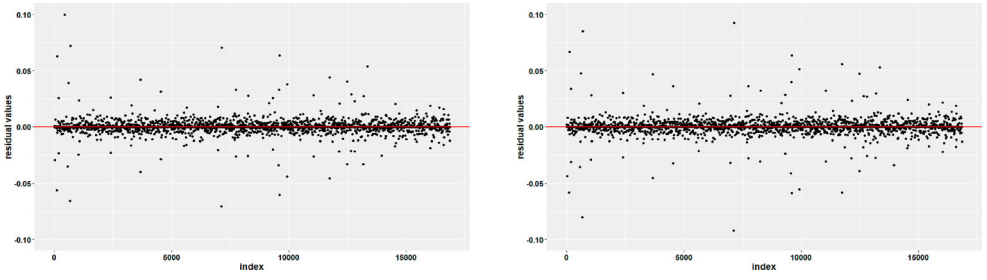


Figure 10. Residual (observed minus predicted) plots for: (*Left*) 2016; (*Right*) 2017.



Figure 11. Year 2016: (*Left*) Risk map; (*Right*) Original data of traffic accidents.



Figure 12. Year 2017: (*Left*) Risk map; (*Right*) Original data of traffic accidents.

4.2. Model prediction

Using the fitted model, we can analyze goodness-of-fit of the model by considering prediction over unsampled locations [79]. This prediction involves projecting the fitted model into the mesh at each road segments.

The proposed model is tested using test years (2016 and 2017) combined with the entire model fitting that used the years 2013 to 2015. From the final predicted result for both test years, we extract monthly predicted values for individual years. In each case, we calculate corresponding residuals of these predictions (observed minus predicted). Figure 10(a ,b) depict such residuals; we note the residuals are generally close to zero and have no



Figure 13. Identified zones having consistent risk value for (*Left*) 2016 and (*Right*) 2017.

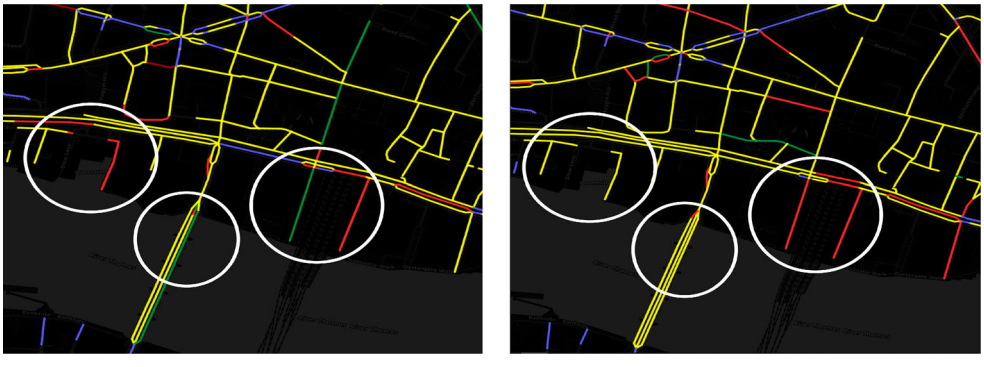


Figure 14. Highlighted streets with upward trend toward higher risk between 2016 (*left*) and 2017 (*right*).

particular structure. Root mean square error (RMSE) value acts as an indicator to assess the performance of a fitted model. We obtained RMSE = 0.0135 for 2016, and RMSE = 0.0121 for 2017, which are similar and particularly small. Further discussion on model performance is reviewed in Section 5.

4.3. Risk map

We calculate the risk index for individual road segments following the indications in Section 3.2, and using the safety measure scale shown in Table 1. The normalized risk index values are calculated using the predicted values for years 2016 and 2017. The risk maps are visualized in an interactive geospatial platform using R package mapview [4]. Figure 11(a) illustrates the risk map for 2016 and corresponding original traffic accident locations are depicted in Figure 11(b). Similar results for 2017 are presented in Figure 12(a ,b). The color scale (0 through 4) used in each map follows the same safety measure scale used in Table 1.

The predicted risk maps are visually compared with original traffic accidents records during the same time span. Some interesting observations are noted. For both years, most of the roads in the outskirts of the city are predicted to be relatively safe than the city center. Indeed, during these years, roads near the city center are predicted with medium to

high risk levels. Figure 13 highlights three consistent risk zones for both years. The leftmost highlighted area being outside the city center shows a steady low risk zone. While the other two highlighted zones represent consistent high risk roads. The identified zones show similar trends when we compare with original accident records during 2016 and 2017.

We note some interesting annual variations in particular road segments identified by our model predictions. If we look at Figure 14, with some streets highlighted by white circles, we see that the predictions from 2016 to 2017 are following an upward trend toward a higher risk. Indeed, the number of accidents in these streets increased from one year to the next.

5. Conclusions and discussion

The current study presents a spatio-temporal model predicting the occurrence of traffic accidents in an urban environment. The model is used to create dynamic risk maps for a road network. To balance computation time and accuracy, the present research work took advantage of the spatio-temporal nature of the data, and used Bayesian methodology by including INLA and SPDE in the modeling process.

Literature [11,39,40] suggests that model fitting using diverse subset combinations of variables provides opportunities to improve prediction accuracy. In the proposed model, we have included three covariates (see Section 2). Out of them, except variables road surface and one of the months (see Table 3 in Appendix) have no influence on the model. Thus, future research works can explain some of the noted variations on improving prediction accuracy by careful inclusion of significant exogenous variables related to traffic flow, traffic control and temporal variables such as time of accident occurrence. Furthermore, studies like [17,50] suggest future research works in exploring reliable and large training data set that can improve the performance of the proposed model.

In recent years, spatio-temporal modeling of road traffic accidents and risk mapping has gained attention, especially in the domain of multi-dimensional road safety management. Besides, travel risk maps are gaining popularity among business travellers, tourists and emergency service providers. Results and findings of the current study illustrate that the proposed model can generate predicted risk maps of the entire road network for any urban study area. In this sense, it is dynamic in nature. The model is flexible and general, and thus can be adapted to similar problems. It can handle different types of covariates in space or time, spatial and temporal structures and space-time interactions. The predicted risk maps of traffic accidents is one of our interesting outcomes. We can produce the road safety index of all road segments, including small details of each junctions or sharp turnings. In our particular problem, we can point to which elements authorities can take dedicated actions to control and reduce traffic accidents as our model identifies significant elements that can be controlled and modified by humans. This means we provide a real, pragmatic and realistic element for institutions to take actions on reducing the risk of traffic accidents.

Moreover, identification of potentially dangerous roads and regions can act as baseline information for geospatial analysis on road safety. The results can have strategic applications in developing GIS analytical tools to identify and depict possible safe routes. As the risk map provides information about the entire road network, it can be flexible enough to generate possible alternative safe route(s) between any source and destinations pairs.

Another important use of the model is analyzing the change and trend pattern of traffic accidents. We can find some literature suggesting this line of research in the city of London [8,15,71], and similar works in other countries [5,34]. As depicted in Figure 14, identification of gradual changes in risk values and their potential factors, are of interest for future research works on change point detection.

Consequently, the novelty of the study is the introduction of *SPDE network triangulation* or *SPDE network mesh* to estimate the spatial auto-correlation of discrete events. As such, it took a new step in INLA-SPDE modeling to perform spatio-temporal predictive analysis only on selected areas (specifically for road networks), instead of performing on entire continuous region. In a broader picture, the study contributes to the relatively small amount of literature on spatio-temporal analysis using INLA-SPDE of spatial events precisely on road networks. The methodology is dynamic and can be adapted and applied to other locations globally.

Author contributions statement

Conceptualization, PJ and SC; Data curation, SC; Formal analysis, SC, PJ and JM; Methodology, SC, PJ and JM; Project administration, JM; Resources, SC; Software, PJ and SC; Validation, PJ and JM; Writing original draft, SC; Writing review & editing, PJ and JM. The authors declare that they have no conflict of interest.

Ethical statement

Author and co-authors testify that, this manuscript is original, has not been published before and is not currently being considered for publication elsewhere. We know of no conflicts of interest associated with this publication and there has been no financial support for this work.

Disclosure statement

No potential conflict of interest was reported by the author(s).

ORCID

Somnath Chaudhuri http://orcid.org/0000-0003-4899-1870
Pablo Juan http://orcid.org/0000-0002-2197-7502
Jorge Mateu http://orcid.org/0000-0002-2868-7604

References

[1] A. Abdel-Salam, F. Guo, A. Flintsch, M. Arafeh, and H. Rakha, *Linear regression crash prediction models*, *Efficient Transportation and Pavement Systems*, CRC Press, 2008.
[2] M. I. Adarabioyo and R. A. Ipinyomi, *Comparing zero-inflated poisson, zero-inflated negative binomial and zero-inflated geometric in count data with excess zero*, Asian J. Probab. Stat. 4 (2019), pp. 1–10.
[3] M. A. Aghajani, R. S. Dezfoulian, A. R. Arjroody, and M. Rezaei, *Applying GIS to identify the spatial and temporal patterns of road accidents using spatial statistics (case study: Ilam Province, Iran)*, Transp. Res. Procedia 25 (2017), pp. 2126–2138.
[4] T. Appelhans, F. Detsch, C. Reudenbach, and S. Woellauer, *mapview – Interactive viewing of spatial data in R*, EGU General Assembly Conference Abstracts, 2016. Article EPSC2016–1832, EPSC2016–1832.
[5] I. Ashraf, S. Hur, M. Shafiq, Y. Park, and Y. Guo, *Catastrophic factors involved in road accidents: Underlying causes and descriptive analysis (Y. Guo, Ed.)*, PLoS. ONE. 14 (2019), pp. e0223473.

[6] E. Azuike, K. Okafor, and P. Okojie, *The causes and prevalence of road traffic accidents amongst commercial long distance drivers in Benin city, Edo state, Nigeria*, Nig. Hosp. Pract. 26 (2017), pp. 220–230.
[7] H. Bakka, H. Rue, G. Fuglstad, A. Riebler, D. Bolin, J. Illian, E. Krainski, D. Simpson, and F. Lindgren, *Spatial modeling with R-INLA: A review*, WIREs Comput. Stat. 10 (2018), pp. e1443.
[8] A. Bhawkar, *Severe traffic accidents in United Kingdom*, Tech. rep., National College of Ireland, 2018. Available at https://www.researchgate.net/publication/330676135_SevereTraffic_Accidents_in_United_Kingdom.
[9] M. Blangiardo and M. Cameletti, *Spatial and Spatio-temporal Bayesian Models with R-INLA*, John Wiley & Sons, Ltd, London, 2015.
[10] Á. Briz-Redón, F. Martínez-Ruiz, and F. Montes, *Identification of differential risk hotspots for collision and vehicle type in a directed linear network*, Accid. Anal. Preven. 132 (2019), pp. 105278.
[11] M. Cameletti, F. Lindgren, D. Simpson, and H. Rue, *Spatio-temporal modeling of particulate matter concentration through the SPDE approach*, AStA Adv. Stat. Anal. 97 (2013), pp. 109–131.
[12] V. Cantillo, P. Garcés, and L. Márquez, *Factors influencing the occurrence of traffic accidents in urban roads: A combined GIS-Empirical Bayesian approach*, DYNA 83 (2016), pp. 21–28.
[13] M. Castro, R. Paleti, and C. R. Bhat, *A latent variable representation of count data models to accommodate spatial and temporal dependence: Application to predicting crash frequency at intersections*, Transp. Res. Part B: Methodol. 46 (2012), pp. 253–272.
[14] S. Chaudhuri, M. Moradi, and J. Mateu, *On the trend detection of time-ordered intensity images of point processes on linear networks*, Commun. Stat. – Simul. Comput. (2021), pp. 1–13. doi: 10.1080/03610918.2021.1881116.
[15] R.P. Curiel, H.G. Ramírez, and S.R. Bishop, *A novel rare event approach to measure the randomness and concentration of road accidents (Y. Deng, Ed.)*, PLoS. ONE. 13 (2018), pp. e0201890.
[16] D. Curran-Everett, *Explorations in statistics: The analysis of ratios and normalized data*, Adv. Physiol. Educ. 37 (2013), pp. 213–219.
[17] E.J. de Fortuny, D. Martens, and F. Provost, *Predictive modeling with big data: Is bigger really better?*, Big. Data. 1 (2013), pp. 215–226.
[18] F. Demasi, G. Loprencipe, and L. Moretti, *Road safety analysis of urban roads: Case study of an Italian municipality*, Safety 4 (2018), pp. 58.
[19] M. Deublein, M. Schubert, B. T. Adey, J. Köhler, and M. H. Faber, *Prediction of road accidents: A Bayesian hierarchical approach*, Accid. Anal. Preven. 51 (2013), pp. 274–291.
[20] C.M. Farmer, *Temporal factors in motor vehicle crash deaths*, Inj. Prev. 11 (2005), pp. 18–23.
[21] U. Galgamuwa, *Bayesian spatial modeling to incorporate unmeasured information at road segment levels with the INLA approach: A methodological advancement of estimating crash modification factors*, J. Traff. Transp. Eng. (English Edition), 2019.
[22] A. Gelman, *Bayesian data analysis*, 2014. [OCLC: 909477393].
[23] Y. Guo, A. Osama, and T. Sayed, *A cross-comparison of different techniques for modeling macro-level cyclist crashes*, Accid. Anal. Preven. 113 (2018), pp. 38–46.
[24] M.-C. Hu, M. Pavlicova, and E.V. Nunes, *Zero-Inflated and hurdle models of count data with extra zeros: Examples from an HIV-Risk reduction intervention trial*, Am. J. Drug. Alcohol. Abuse. 37 (2011), pp. 367–375.
[25] J. Huang, B. P. Malone, B. Minasny, A. B. McBratney, and J. Triantafilis, *Evaluating a Bayesian modelling approach (INLA-SPDE) for environmental mapping*, Sci. Total Environ. 609 (2017), pp. 621–632.
[26] F.J. Jegede, *Spatio-temporal analysis of road traffic accidents in Oyo state, Nigeria*, Accid. Anal. Prev. 20 (1988), pp. 227–243.
[27] P. Juan, J. Mateu, and M. Saez, *Pinpointing spatio-temporal interactions in wildfire patterns*, Stoch. Environ. Res. Risk. Assess. 26 (2012), pp. 1131–1150.
[28] M. Karacasu, B. Ergül, and A.A. Yavuz, *Limited. estimating the causes of traffic accidents using logistic regression and discriminant analysis*, Int. J. Inj. Contr. Saf. Promot. 21 (2013), pp. 305–313.

[29] A. Karaganis, *A Spatial Point Process for Estimating the Probability of Occurrence of a Traffic Accident*, European Regional Science Association, ERSA conference papers, 2006.
[30] D. Khulbe, *Modeling Severe Traffic Accidents With Spatial And Temporal Features*, ICONIP, 2019.
[31] D. Lambert, *Zero-Inflated poisson regression, with an application to defects in manufacturing*, Technometrics 34 (1992), pp. 1–14.
[32] F. Lindgren, H. Rue, and J. Lindström, *An explicit link between Gaussian fields and Gaussian Markov random fields: The stochastic partial differential equation approach*, J. R. Stat. Soc.: Ser. B (Stat. Methodol.) 73 (2011), pp. 423–498.
[33] C. Liu, *Exploring spatio-temporal effects in traffic crash trend analysis*, Anal. Meth. Accid. Res. 16 (2017), pp. 104–116.
[34] C. Liu, S. Zhang, H. Wu, and Q. Fu, *A dynamic spatiotemporal analysis model for traffic incident influence prediction on urban road networks*, ISPRS Int. J. Geo-Inform. 6 (2017), pp. 362.
[35] B.P.Y. Loo, S. Yao, and J. Wu, *Spatial point analysis of road crashes in Shanghai: A GIS-based network kernel density method*, 2011 19th International Conference on Geoinformatics, 2011.
[36] A. Lopez-Quilez and F. Munoz, *Review of spatio-temporal models for disease mapping*, Tech. rep., 2009. Available at https://www.uv.es/famarmu/doc/Euroheis2-report.pdf.
[37] D. Lord and B. N. Persaud, *Accident prediction models with and without trend: Application of the generalized estimating equations procedure*, Transp. Res. Rec.: J. Transp. Res. Board 1717 (2000), pp. 102–108.
[38] R. Lovelace and R. Ellison, *stplanr: A package for transport planning*, The R Journal 10 (2018), pp. 7–23.
[39] J. Martínez-Minaya, F. Lindgren, A. López-Quílez, D. Simpson, and D. Conesa, *The Integrated nested Laplace approximation for fitting models with multivariate response*, 2021.
[40] S. Martino and H. Rue, *Case studies in Bayesian computation using INLA*, in *Complex Data Modeling and Computationally Intensive Statistical Methods*, P. Mantovan, P. Secchi, eds., Springer, Milan, 2010. pp. 99–114.
[41] T. G. Martins, D. Simpson, F. Lindgren, and H. Rue, *Bayesian computing with INLA: New features*, Comput. Stat. Data Anal. 67 (2013), pp. 68–83.
[42] S.-P. Miaou, *The relationship between truck accidents and geometric design of road sections: Poisson versus negative binomial regressions*, Accid. Anal. Preven. 26 (1994), pp. 471–482.
[43] M. Miler, F. Todić, and M. Sevrović, *Extracting accurate location information from a highly inaccurate traffic accident dataset: A methodology based on a string matching technique*, Transp. Res. Part C: Emerg. Technol. 68 (2016), pp. 185–193.
[44] M. Mohanty and A. Gupta, *Factors affecting road crash modeling*, J. Transp. Lit. 9 (2015), pp. 15–19.
[45] M.M. Moradi, *Spatial and spatio-temporal point patterns on linear networks*, Doctoral diss., Universitat Jaume I, 2018.
[46] M.M. Moradi and J. Mateu, *First- and second-order characteristics of spatio-temporal point processes on linear networks*, J. Comput. Graph. Stat. 0 (2019), pp. 1–21.
[47] P. Moraga, *Geospatial Health Data : Modeling and Visualization with R-INLA and Shiny*, CRC Press, London, 2020.
[48] NCHRP, *Quality and Accuracy of Positional Data in Transportation*, Transportation Research Board, 2003.
[49] J. Oh, S. P. Washington, and D. Nam, *Accident prediction model for railway-highway interfaces*, Accid. Anal. Preven. 38 (2006), pp. 346–356.
[50] M.C.M. Oo and T. Thein, *An efficient predictive analytics system for high dimensional big data*, J. King Saud University – Comput. Inform. Sci. 34 (2019), pp. 1521–1532.
[51] M. Padgham, B. Rudis, R. Lovelace, and M. Salmon, *OSM Data*, The J. Open Source Softw. 2 (2017), 305.
[52] V. Prasannakumar, H. Vijith, R. Charutha, and N. Geetha, *Spatio-Temporal clustering of road accidents: GIS based analysis and assessment*, Procedia – Soc. Behav. Sci. 21 (2011), pp. 317–325.
[53] S.S. Pulugurtha and V.R. Sambhara, *Pedestrian crash estimation models for signalized intersections*, Accid. Anal. Preven. 43 (2011), pp. 439–446.

[54] Risk mapping for the TEN-T in Croatia, Greece, Italy and Spain: Update. *EuroRAP* 2016. Available at https://eurorap.org/risk-mapping-for-the-ten-t-in-croatia-greeceitaly-and-spain-update/.
[55] C.E. Rose, S.W. Martin, K.A. Wannemuehler, and B.D. Plikaytis, *On the use of zero-inflated and hurdle models for modeling vaccine adverse event count data*, J. Biopharm. Stat. 16 (2006), pp. 463–481.
[56] H. Rue and L. Held, *Gaussian Markov Random Fields: Theory and Applications (Chapman & Hall/CRC Monographs on Statistics and Applied Probability)*, Chapman & Hall/CRC, London, 2005.
[57] H. Rue, S. Martino, and N. Chopin, *Approximate Bayesian inference for latent Gaussian models by using integrated nested Laplace approximations*, J. R. Stat. Soc.: Ser. B (Stat. Methodol.) 71 (2009), pp. 319–392.
[58] H. Rue, A. Riebler, S.H. Sørbye, J.B. Illian, D.P. Simpson, and F.K. Lindgren, *Bayesian Computing with INLA: A Review*, 2016.
[59] H. Rue, A. Riebler, S.H. Sørbye, J.B. Illian, D.P. Simpson, and F.K. Lindgren, *Bayesian computing with INLA: A review*, Annu. Rev. Stat. Appl. 4 (2017), pp. 395–421.
[60] M. Salifu, *Accident prediction models for unsignalised urban junctions in Ghana*, IATSS Res. 28 (2004), pp. 68–81.
[61] L. Serra, M. Saez, P. Juan, D. Varga, and J. Mateu, *A spatio-temporal Poisson hurdle point process to model wildfires*, Stoch. Environ. Res. Risk. Assess. 28 (2013), pp. 1671–1684. doi: 10.1007/s00477-013-0823-x.
[62] G. A. Shafabakhsh, A. Famili, and M. S. Bahadori, *GIS-based spatial analysis of urban traffic accidents: Case study in Mashhad, Iran*, J. Traffic Transp. Eng. (English Edition) 4 (2017), pp. 290–299.
[63] S. Shahid, A. Minhans, O. Che Puan, S. A. Hasan, and T. Ismail, *Spatial and temporal pattern of road accidents and casualties in peninsular Malaysia*, J. Teknol. 76 (2015), pp. 000.
[64] D.P. Simpson, H. Rue, A. Riebler, T.G. Martins, and S.H. Sørbye, *Penalising model component complexity: A principled, practical approach to constructing priors*, preprint (2014), arXiv doi: 10.48550/ARXIV.1403.4630.
[65] D. Simpson, H. Rue, A. Riebler, T.G. Martins, and S.H. Sørbye, *Penalising model component complexity: A principled, practical approach to constructing priors*, Stat. Sci. 32 (2017), pp. 1–28.doi: 10.1214/16-sts576.
[66] T.D. Smedt, *Comparing MCMC and INLA for disease mapping with Bayesian hierarchical models*, Arch. Public Health 73 (2015), doi: 10.1186/2049-3258-73-s1-o2.
[67] D. J. Spiegelhalter, N. G. Best, B. P. Carlin, and A. van der Linde, *Bayesian measures of model complexity and fit*, J. R. Stat. Soc.: Ser. B (Stat. Methodol.) 64 (2002), pp. 583–639.
[68] B.M. Taylor and P.J. Diggle, *INLA or MCMC? A tutorial and comparative evaluation for spatial prediction in log-Gaussian Cox processes*, J. Stat. Comput. Simul. 84 (2014), pp. 2266–2284.
[69] TFL, *Transport for London: Road Safety*, 2019. Retrieved April 30, 2019, Available at https://tfl.gov.uk/corporate/publications-and-reports/road-safety.
[70] P.J. Verdoy, *Enhancing the SPDE modeling of spatial point processes with INLA, applied to wildfires. choosing the best mesh for each database*, Commun. Stat. – Simul. Comput. 50 (2021), pp. 2990–3030.
[71] C. Wang, M. A. Quddus, and S. G. Ison, *Impact of traffic congestion on road accidents: A spatial analysis of the M25 motorway in England*, Accid. Anal. Prev. 41 (2009), pp. 798–808.
[72] W. Wang, Z. Yuan, Y. Yang, X. Yang, Y. Liu, and Y. Guo, *Factors influencing traffic accident frequencies on urban roads: A spatial panel time-fixed effects error model (Y. Guo, Ed.)*, PLoS. ONE. 14 (2019), pp. e0214539.
[73] S. Watanabe, *Asymptotic equivalence of Bayes cross validation and widely applicable information criterion in singular learning theory*, J. Mach. Learn. Res. 11 (2010), 3571–3594.
[74] WHO, *Global Status Report on Road Safety 2018*, World Health Organization, (2019, Jan 10).
[75] C. K. Wikle, L. M. Berliner, and N. Cressie, *Hierarchical Bayesian space-time models*, Environ. Ecol. Stat. 5 (1998), pp. 117–154.

[76] A. M. Williamson and A.-M. Feyer, *Causes of accidents and the time of day*, Work & Stress 9 (1995), pp. 158–164.
[77] P. Xu and H. Huang, *Modeling crash spatial heterogeneity: Random parameter versus geographically weighting*, Accid. Anal. Prev. 75 (2015), pp. 16–25.
[78] F. Zhong-xiang, L. Shi-sheng, Z. Wei-hua, and Z. Nan-nan, *Combined prediction model of death toll for road traffic accidents based on independent and dependent variables*, Comput. Intell. Neurosci. 2014 (2014), pp. 1–7.
[79] A.F. Zuur, *Beginners Guide to Spatial, Temporal and Spatial-Temporal Ecological Data Analysis with R-INLA: Using GLM and GLMM (Vol. 1)*, Highland Statistics Ltd, Scotland, 2017.